A comparative study of system size dependence of the effect of non-unitary channels on different classes of quantum states

Geetu Narang*
Department of Applied Sciences, U.I.E.T, Panjab University, Chandigarh 160040, India

Shruti Dogra† and Arvind‡
Department of Physics, Indian Institute of Science Education and Research, Mohali, India§

We investigate the effect of different types of non-unitary quantum channels on multi-qubit quantum systems. For an n-qubit system and a particular channel, in order to draw unbiased conclusions about the system as a whole as opposed to specific states, we evolve a large number of randomly generated states under the given channel. We increase the number of qubits and study the effect of system size on the decoherence processes. The entire scheme is repeated for various types of environments which include dephasing channel, depolarising channel, collective dephasing channel and zero temperature bath. Non-unitary channels representing the environments are modeled via their Karus operator decomposition or master equation approach. Further, for a given n we restrict ourselves to the study of particular subclasses of entangled states, namely the GHZ-type and W-type states. We generate random states within these classes and study the class behaviors under different quantum channels for various values of n.

PACS numbers: -03.65.Xp,03.65.Aa

I. INTRODUCTION

Inability to overcome the effects of decoherence is the most crucial hurdle in quantum information processing [1, 2]. Hence one of the fundamental requirements to build a quantum computer is to understand and control the process of decoherence. Several platforms have been proposed for scalable implementation of quantum computers on the basis of superconductors [3], semiconductors [4], ion traps [5], spins in solids [6, 7] and spins of molecules using NMR techniques [8, 9]. In all the platforms, decoherence time scales are typically estimated for individual qubits whereas practical implementation of a quantum computer requires the use of many qubits. For multiqubit systems, correlations between qubits can arise and Hilbert space dimension grows exponentially with number of qubits. Estimating the decoherence costs and effect of decohering environments on entanglement for multiqubit systems has also been investigated by several authors [10–13]. Since new ways in which decoherence can effect the system can emerge for multiqubit systems, investigation of the behavior of the system with increased number of qubits is important.

The non-unitary environmental effects can be classified as dissipation and dephasing. While dissipation involves energy exchange and is possible at the classical level too, dephasing is a purely quantum mechanical phenomena [14]. In any case both lead to information loss and state degradation. If we consider system and the environment as a whole, their dynamics is unitary. The environment by its very nature is inaccessible, and to obtain the dynamics of the system alone we can trace over the environment. This may lead to a non-unitary evolution of the system. At a fundamental level, environment induced non-unitary processes are completely positive maps and such maps allows a representation via Karus operators as follows [15]:

$$\rho^{\rm out} = E(\rho) = \sum_{\nu=1}^{N} K_\nu^\dagger \rho K_\nu \quad \text{with} \quad \sum_\nu K_\nu^\dagger K_\nu = 1, \quad (1)$$

where K_ν are the Kraus operators. This evolution is in general non-unitary leading to decoherence, however, the unitary quantum evolution is included and corresponds to a situation when only one of the Kraus operators is non-zero. Depending upon the kinds of Kraus operators involved the channels are classified. In our analysis depolarising channel and collective dephasing channels will be described through their Kraus operators.

Sometimes a channel is described in terms of an explicit environmental model, which when environment is traced out gives us a non-unitary channel. This channel is represented by Lindblad master equation whose solution provides us with time evolution of the system [16]. In this approach we start with the total Hamiltonian of the system together with the environment which has a general form:

$$H = H_S + H_E + V \quad (2)$$

where H_S is the system Hamiltonian, H_E is the environment or the bath Hamiltonian and V is the interaction Hamiltonian. For a particular kind of environment, beginning with the total Hamiltonian of the system we obtain the equation governing the dynamics of the system

* geet29@gmail.com
† shrutidogra@iisermohali.ac.in
‡ arvind@iisermohali.ac.in
§ QTF Centre of Excellence, Department of Applied Physics, Aalto University School of Science, P.O. Box 15100, FI-00076 AALTO, Finland

density operator alone called the master equation [17, 18]. We will employ this method while dealing with the channel termed “zero temperature bath” and dephasing channel.

Our aim in this work is to study the behavior or quantum systems under different non-unitary processes with a focus on its dependence on the system size. Under a given non-unitary channel, different states of a system behave differently. In order to draw conclusion about the system as a whole we generate a large number of random states and average our results over this sample set. Assuming that we have a large enough sample set and the sampling of the state space is uniform our conclusions pertain to the system as a whole and are state independent. For an n-qubit system, we take a particular channel and see its effect as we change the values of n. Then we repeat the exercise for another channel. This allows us to analyze the size dependences of the effect of these non-unitary channels and make comparisons of these effects across different channels in a state independent manner. Channels that we consider include, zero temperature bath, dephasing channel, collective dephasing channel and depolarising channel

In a similar vain for the n-qubit Hilbert space(for $n > 1$) we consider entangled states and study their decoherence properties under four decoherening channels that we considered for the earlier study. Motivated by the structure of different inequivalent maximally entangled states for three qubits namely the GHZ and W states we define “GHZ-type” and “W-type” states for systems with $n > 1$. We study these families separately and make comparisons about their decoherence under various channels. We find very interesting comparisons and contrasts in the behavior. Throughout, while studying a particular class of states we generate a large number of samples in that particular class and average the behavior over these samples to obtain state independent results as was done for the full n-qubit state space.

The effect of decoherence can be estimated by computing the change in the state that takes place due to the environmental factors. For the case where we start with an initial pure state, a good measure of deviation is fidelity defined in terms of the overlap of the initial pure state $|\psi_0\rangle$ and the final mixed or pure state ρ^{out}.

$$F = \langle\psi|\rho^{\text{out}}|\psi\rangle. \tag{3}$$

Fidelity can take values between 0 and 1 and the deviation from 1 indicates the amount of degradation or change.

The computations involve a mix of analytical and numerical tools. The general forms of output states are computed analytically and then numerical simulations are carried out on randomly generated states from the family of states under consideration. The uniform distribution is achieved by the appropriate use of pseudo random function of Mathematica. We observe that, in the case of zero temperature bath channel, degradation rate with respect to number of qubits is maximum in case of W-type states and minimum in case of GHZ-type states. The rate of degeneration in case of dephasing channel is minimum for GHZ-type states and maximum for general states. Depolarising channel destroys all the three sets of states in a similar way. In the case of collective dephasing channel, degeneration rate of the state with respect to system size is negligible for GHZ-type states, whereas it is very similar for general states and W-type states. We have also computed and displayed the fidelity distributions for different classes of states, under different channels and their variation with number qubits.

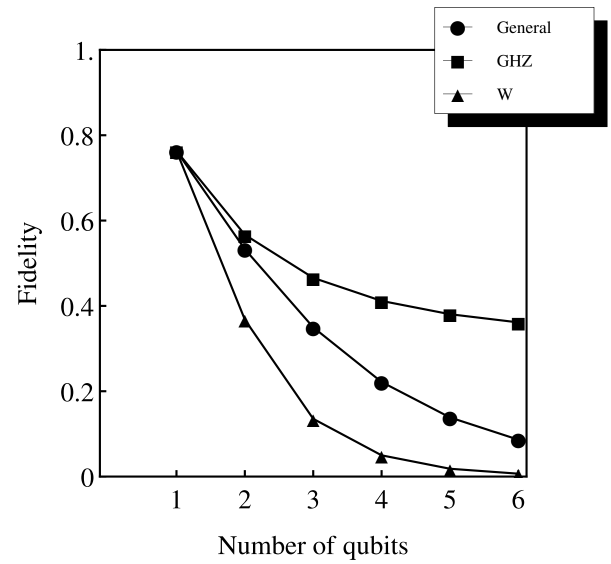

FIG. 1. Variation of average fidelity for $n = 1$ to 6 qubits for zero temperature bath model. Input states are general states, GHZ-type states and W-type-states. The value of $\gamma_1 t = 1$. As can be seen the W-type states degeneration much faster than the GHZ-type states and general states.

The paper is organized as follows: In Section II we define the three classes of states namely, the general states, the GHZ-type states and the W-type states. We then define and discuss the four non-unitary channels, the zero temperature bath, the dephasing channel, the collective dephasing channel and the depolaring channel and the evolution of the family of states under these channels. The results are shown as average fidelities as a function of number of qubits for different state classes for a given channel. We also display the fidelity distributions. In Section III we compare the effects of all four channels on each set of state classes. Here the graphs of average fidelity as a function of the number of qubits are shown for a given class of states for all four non-unitary channels. Section IV offers some concluding ramarks.

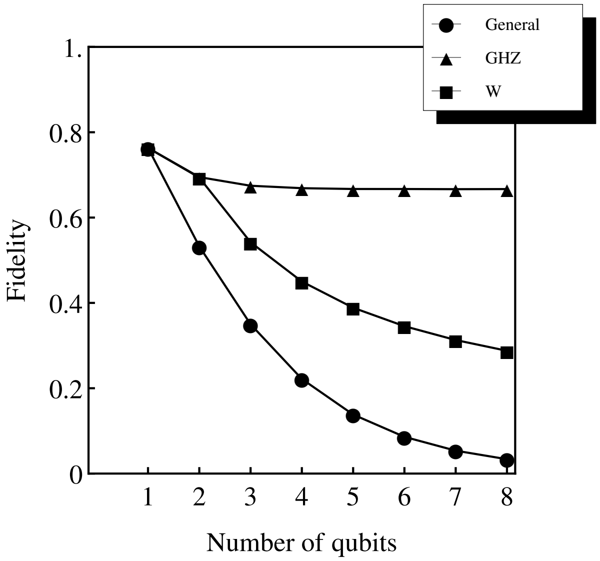

FIG. 2. Variation of average fidelity as a function of system size for the dephasing channel. Fidelity is calculated for general, GHZ-type and W-type states. The value of $\gamma_2 \mathrm{t} = 2.48$

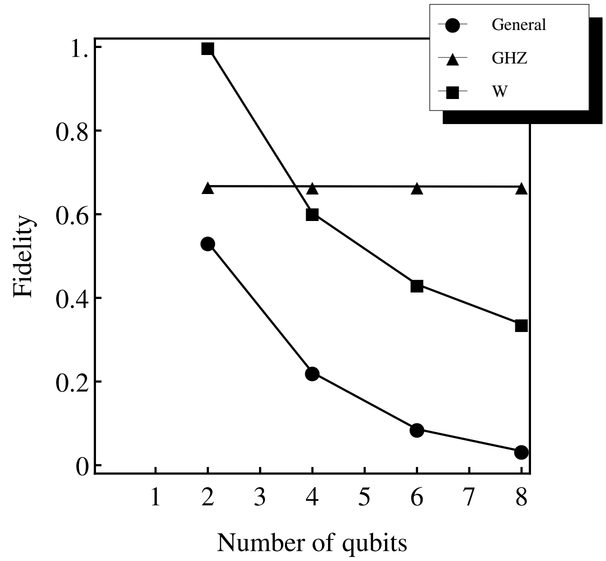

FIG. 3. Variation of average fidelity as a function of system size for collective dephasing channel for $\Gamma \mathrm{t} = 5$. The input states are general states, general GHZ state and W-type state.The degeneration of general states is maximum whereas GHZ-type states do not show any decrease in fidelity with increase in system size.

II. CLASSES OF STATES AND THEIR EVOLUTION UNDER DIFFERENT CHANNELS

In this section we describe our main results where we study certain families of states of an n-qubit system under different non-unitary channels. For $n = 1$ we have only one class of states which are the most general states of the system. For an $n > 1$ we consider three types of states, namely the general states, GHZ-type states and W-type states. The latter two types are motivated by the structure of superpositions involved in the two inequivalent classes of maximally entangled states for three qubits. These families are defined as below:

(a) **General states:** For an n-qubit system, the most general state can be expressed as a linear combination of all the computational basis states as follows:

$$\begin{aligned} \mid \psi_{\text{General}} \rangle = \alpha_0 \mid 000....0\rangle + \alpha_1 \mid 000...1\rangle + \\ \alpha_2 \mid 000...10\rangle ....\alpha_{2^n-1} \mid 111......1\rangle \end{aligned} \tag{4}$$

where α_0, $\alpha_1......\alpha_{2^n-1}$ complex numbers satisfying $\sum_{j=0}^{2^n-1} |\alpha_j|^2 = 1$

(b) **GHZ-type states:** A GHZ-type state for an n-qubit system is defined as follows:

$$\mid \psi_{\text{GHZ}} \rangle = \alpha \mid 000.....0\rangle + \beta \mid 111.....1\rangle \tag{5}$$

where α and β can have any complex numbers with $|\alpha|^2 + |\beta|^2 = 1$.

(c) **W-type states:** A W-type state is defined as follows:

$$\begin{aligned} \mid \psi_{\text{W}} \rangle = \beta_1 \mid 000......001\rangle + \beta_2 \mid 000.....010\rangle + \\ \beta_3 \mid 000...0100\rangle + ... + \beta_n \mid 1000......000\rangle; \end{aligned} \tag{6}$$

where β_1,β_2 .... β_n again complex number with $\sum_{j=1}^{n} |\beta_j|^2 = 1$.

We are now ready to study the effect of different non-unitary channels on the classes of states define above. We will start with a single qubit and try to go up to 8 qubits.

A. Channel with zero temperature bath as environment

For the non-unitary process were we have a zero temperature bath of qubits in the environment, we assume that each qubit interacts with the bath qubits independently. We consider the Lindblad master equation for the evolution of the system density operator ρ to model the interaction the system with the bath, given as [17]:

$$\frac{d\rho}{dt} = \sum_{k=1}^{n} (I \otimes ...... \otimes L_k \otimes ...... \otimes I)\rho. \tag{7}$$

Here L_k is a single qubit operator and is defined by its action on the kth qubit in terms of Pauli operators $\sigma_{\pm} = \sigma_1 \pm i\sigma_2$ as:

$$L_k \rho_k = \frac{\gamma_1}{2}(2\sigma_- \rho_k \sigma_+ - \sigma_+ \sigma_- \rho_k - \rho_k \sigma_+ \sigma_-) \tag{8}$$

The parameter γ_1 depends upon the strength of the system bath interaction.

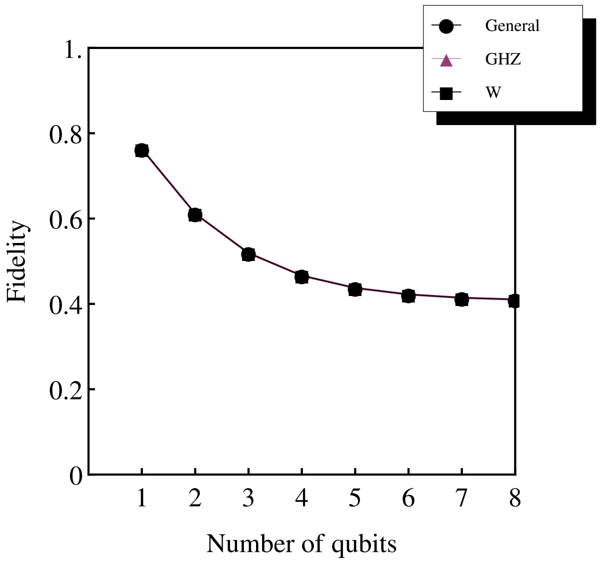

FIG. 4. Average fidelity as a function of system size for depolarising channel for the value p = 0.8348. The input states include general states, GHZ-type states and W-type states.

For the $n = 1$ case, let the initial state of the system be $\rho = |\psi_0\rangle\langle\psi_0|$. Then the final state obtained at time t by solving Equation (7) is given as

$$\rho^{\text{out}} = \begin{pmatrix} e^{-t\gamma_1}\rho_{11} & e^{-t\gamma_1/2}\rho_{12} \\ e^{-t\gamma_1/2}\rho_{21} & (1-e^{-t\gamma_1})\rho_{11}+\rho_{22} \end{pmatrix} \tag{9}$$

where $\rho_{ij} = \langle i|\rho|j\rangle$ is the i, j^{th} element of the initial state ρ in the computational basis. Since, both diagonal as well as off-diagonal terms are being affected by the channel, it is clear that the interaction of the system with the bath results in both dissipation and decoherence of the state. Similarly final states for the systems upto 6 qubits can be calculated analytically. The expressions are long and therefore are not being displayed. As $t \to \infty$, the decohered state in Equation (9) approaches the lower energy state with $\rho_{22}^{\text{out}} = \rho_{11} + \rho_{22} = 1$. This happens for higher number of qubits too and is a reflection of the fact that we are working with a zero temperature bath.

Once we have the final state the fidelity can be calculated using Equation (3). We generate 100,000 random states numerically and compute the fidelity and the average fidelity. The process is repeated for upto 6 qubits. Next for $n > 1$ we restrict ourselves to GHZ-type and W-type states and again generate random states and compute average fidelity. The average fidelities are shown in Figure 1. All fidelities are computed for $\gamma_1 t = 1$. The histograms of fidelities are shown in Figures 5, 6 & 7 where first column in each figure corresponds to the zero temperature bath channel.

The difference in degeneration properties of the three classes of states are clearly visible in Figure 1. While the W-type states degeneration more rapidly compared to general states GHZ-type states are more robust. Another interesting result obtained while calculating the fidelities for W-type states is that all states in W-type family have same fidelity It implies that in case system is interacting with a zero temperature bath, all the n-qubit states in W-state space degeneration in exactly the same way. This is clearly seen from the first column of Figure 7. The 1st columns of Figures 5,6 & 7 show how the fidelities are distributed, for general, GHZ-type and W-type states repectively. The fidelity distribution is most broad for the GHZ-type states and for general states the distribution tends to become narrow as the number of qubits increases.

B. Dephasing channel

Dephasing channel destroys the off-diagonal elements of a density matrix which correspond to coherences among the computational basis states [19, 20]. In this case like the zero temperature bath, the qubits interact with the environment individually and we use the master equation model described in Equation (7). Lindblad operator in this case is again given through its action on single qubit density operator in terms of Pauli matrices as:

$$L_k\rho_k = \frac{\gamma_2}{2}(2\sigma_-\sigma_+\rho_k\sigma_-\sigma_+ - \sigma_-\sigma_+\sigma_-\sigma_+\rho_k - \rho_k\sigma_-\sigma_+\sigma_-\sigma_+) \tag{10}$$

Here γ_2 depends upon the interaction strength between the system and the bath. Using the similar procedure as used in the zero temperature bath case, we obtain the final density matrix for the state under dephasing channel for a single qubit

$$\rho^{\text{out}} = \begin{pmatrix} \rho_{11} & e^{-t\gamma_2/2}\rho_{12} \\ e^{-t\gamma_2/2}\rho_{21} & \rho_{22} \end{pmatrix} \tag{11}$$

It is clear from the RHS of the above equation that that the channel affects only the off diagonal terms whereas the diagonal terms remains unaffected. The final state for $n > 1$ can be calculated and have similar structure, however we are not displaying the long expression. The analytical expressions for fidelity upto eight qubits can be obtained using the final density matrices. Generating a large number of random states, as in case of zero temperature bath, we obtain the fidelity distributions for all three classes of states for $n = 1$ to $n = 8$. The average fidelities are shown in Figure 2 while the histograms of fidelities are shown in the second columns of Figures 5,6 & 7. Comparison of the average Fidelities of three set of states is shown in Figure 2 reveals how classes are affected by the channel. Decoherence of GHZ-type states is minimum and the decoherence of general states is maximum. This quite different from the zero temperature bath.

We can attribute the slow decoherence of GHZ-type states and W-type states in comparison to general states to the number of phases involved in both the GHZ and W type states. Number of relative phases in case of GHZ-type states is just one, therefore it has only one way to degrade. In case of W-type states, more relative phases are involved, therefore, W-type states degeneration relatively more in comparison to GHZ-type states. Number of relative phases goes up with number of qubits in case of general states, therefore, degeneration is drastic. An important observation about the GHZ-type states is that their fidelity converges to 0.66 as the number of qubits increases.

Looking at the second columns of Figures 5,6 & 7 we can see how the fidelities are distributed. Again the Fidelity distributions are very different for the three classes of states and very different from the zero temperature bath.

C. Collective dephasing channel

The collective dephasing channel is similar to dephasing channel. However For its action we need at least two qubits which are collectively coupled to an environment. This channel can be described using the Kraus operators as follows [21]:

$$\begin{aligned}
D_1 &= \begin{pmatrix} \gamma_3(t) & 0 & 0 & 0 \\ 0 & 1 & 0 & 0 \\ 0 & 0 & 1 & 0 \\ 0 & 0 & 0 & \gamma_3(t) \end{pmatrix}, \quad \gamma_3(t) = e^{-\frac{t}{2T}} \\
D_2 &= \begin{pmatrix} \omega_1(t) & 0 & 0 & 0 \\ 0 & 0 & 0 & 0 \\ 0 & 0 & 0 & 0 \\ 0 & 0 & 0 & \omega_2(t) \end{pmatrix}, \quad \begin{matrix} \omega_1(t) = \sqrt{1 - e^{\frac{-t}{T}}} \\ \omega_2(t) = -e^{-t/T}\sqrt{1 - e^{\frac{-t}{T}}} \end{matrix} \\
D_3 &= \begin{pmatrix} 0 & 0 & 0 & 0 \\ 0 & 0 & 0 & 0 \\ 0 & 0 & 0 & 0 \\ 0 & 0 & 0 & \omega_3(t) \end{pmatrix}, \quad \omega_3(t) = \sqrt{(1 - e^{-\frac{t}{T}})(1 - e^{-\frac{2t}{T}})}.
\end{aligned} \tag{12}$$

The phase relaxation time T due to the collective interaction of the system with the bath which is the inverse of the damping rate Γ of the system is the single parameter characterizing the channel. The action of the channel on a general two qubit quantum state ρ is given as:

$$\rho^{\rm out} = \sum_{j=1}^{3} D_j^\dagger \rho D_j. \tag{13}$$

Since collective dephasing channel acts on two qubits at a time, we have considered even number of qubits namely 2,4,6 and 8 in our analysis. Once again, beginning with a general pure state of two qubits we let it evolve under the channel defined in Equation (13) and evaluate the output state, which turns out to be:

$$\rho^{\rm out} = \begin{pmatrix} (\gamma_3^2 + {\omega_1}^2)\rho_{11} & \gamma_3\rho_{12} & \gamma_3\rho_{13} & (\gamma_3^2 + \omega_1\omega_2)\rho_{14} \\ \gamma_3\rho_{21} & \rho_{22} & \rho_{23} & \gamma_3\rho_{24} \\ \gamma_3\rho_{31} & \rho_{32} & \rho_{33} & \gamma_3\rho_{34} \\ (\gamma_3^2 + \omega_1\omega_2)\rho_{41} & \gamma_3\rho_{42} & \gamma_3\rho_{43} & (\gamma_3^2 + \omega_2^2 + \omega_3^2)\rho_{44} \end{pmatrix} \tag{14}$$

The expression of the final state shows that the 2-3 subspace corresponding the "zero quantum" is not effected at all. This interesting feature is reflected in Figure 3, where, for $n = 2$, the average fidelity in the case of W-type state is 1 while it is much smaller values for GHZ-type and general states. The final states corresponding to 4, 6 and 8 qubits can be calculated in a similar way and from the final state we can calculate the fidelity. Again we generate a large number random states within the same three classes and compute the distribution of fidelities. The average fidelities are shown in Figure 3 while the fidelity distributions are shown in the third columns of Figures 5,6 & 7.

The average fidelity degeneration behaviors with chanding n shown in Figure 3 is similar to that of dephasing channel. Decay of GHZ-type states in comparison to general states and W-type states is minimum. The change in the degeneration rate of GHZ-type states is very small as we increase number of qubits. General states are more fragile compared to the other two families and increase in their degeneration rate is fastest with respect to the number of qubits. As was explained in the case of dephasing channel, states degeneration depending on the number of relative phases contained in them. GHZ-type states contain minimum number of phases, therefore degeneration is minimum. General states contain maximum number of phases, therefore maximum degeneration in their case. The general pattern of fidelity distributions shown in the third columns of Figures 5,6 & 7 shows that overall the behaviors is similar to the dephasing channel.

D. Depolarising channel

Depolarising channel describe the system environment interaction in the large temperature regime. There are ways to obtain this channel from explicit models of such interactions in the high temperature limit, however, we directly use the model of this channel using the Kraus operators. For a single qubit a general Pauli channel has its Kraus operators represented by Pauli matrices $\sigma_j, j = 1, 2, 3$ as follows:

$$\epsilon(\rho) = p_0\rho + \sum_{i=1}^{3} p_i\sigma_i\rho\sigma_i \tag{15}$$

where $p_i \geq 0$, $p_0+p_1+p_2+p_3 = 1$. When $p_1 = p_2 = p_3$ the above channel corresponds to the depolarising channel. The depolarising channel therefore, can be represented

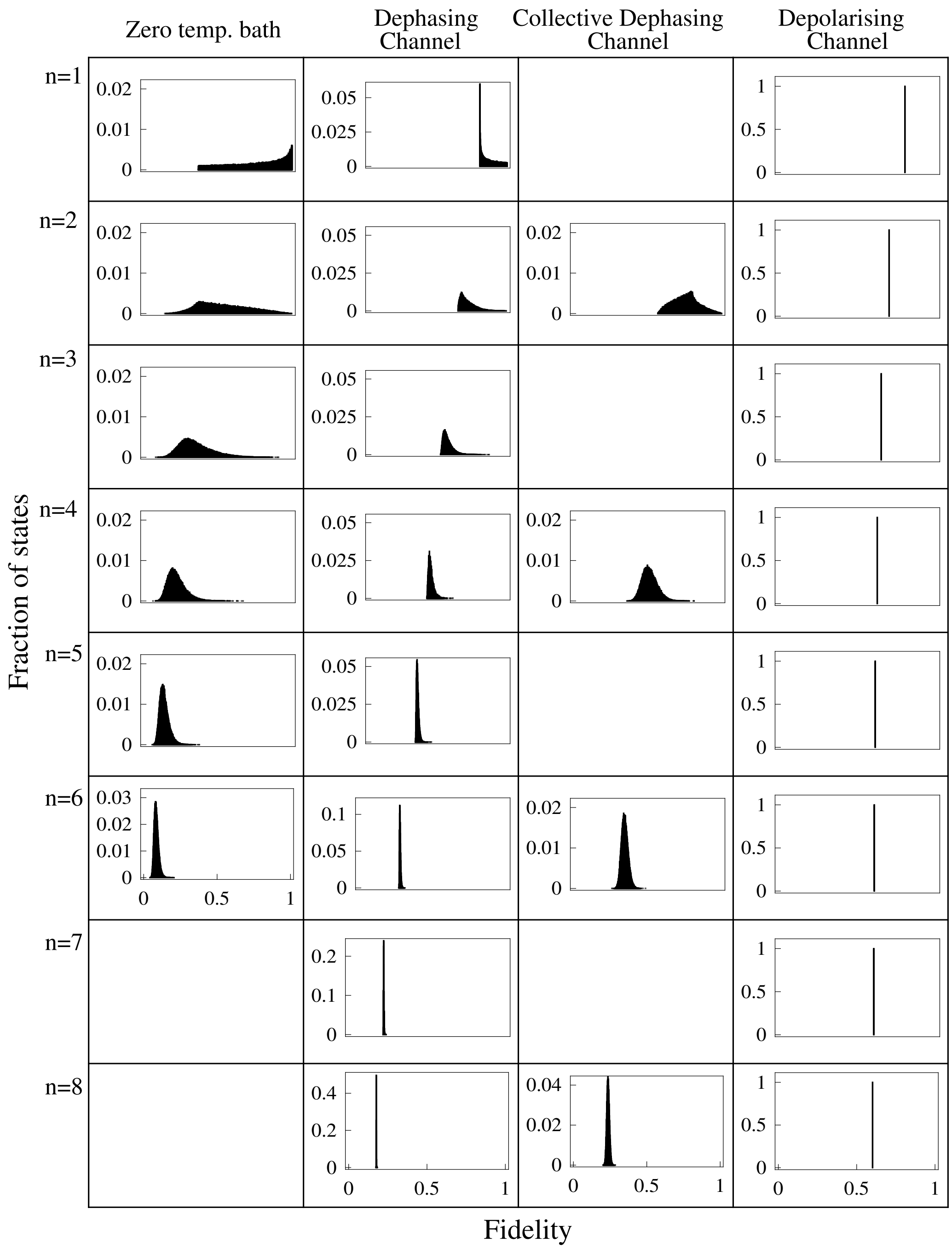

FIG. 5. Fidelity distribution of uniformly distributed random general states as a function of system size. The variance of Fidelity distribution is maximum in case of zero temperature bath and is minimum in case of depolarising channel. The Fidelity distributions of dephasing and collective dephasing channel show similar behavior with increasing number of qubits.

by a single parameter p as follows:

$$\rho^{\text{out}} = E(\rho) = (1-p)\rho + \frac{p}{3}(\sigma_1\rho\sigma_1 + \sigma_2\rho\sigma_2 + \sigma_3\rho\sigma_3). \quad (16)$$

For single qubit state the action of the depolarising channel can be computed using Equation (16) resulting in the transformation of input ρ to the output state ρ^{out} with

$$\rho^{\text{out}} = \begin{pmatrix} -\frac{1}{2}(-2+p)\rho_{11} & -(-1+p)\rho_{12} + \frac{1}{2}p\rho_{21} \\ -(-1+p)\rho_{21} + \frac{1}{2}p\rho_{12} & -\frac{1}{2}(-2+p)\rho_{22} \end{pmatrix} \quad (17)$$

Since the depolarising channel effects both the diagonal and off diagonal terms of the state, it results in both decoherence and dissipation of the system. The effect of a depolarising channel on states for $n > 1$ can be

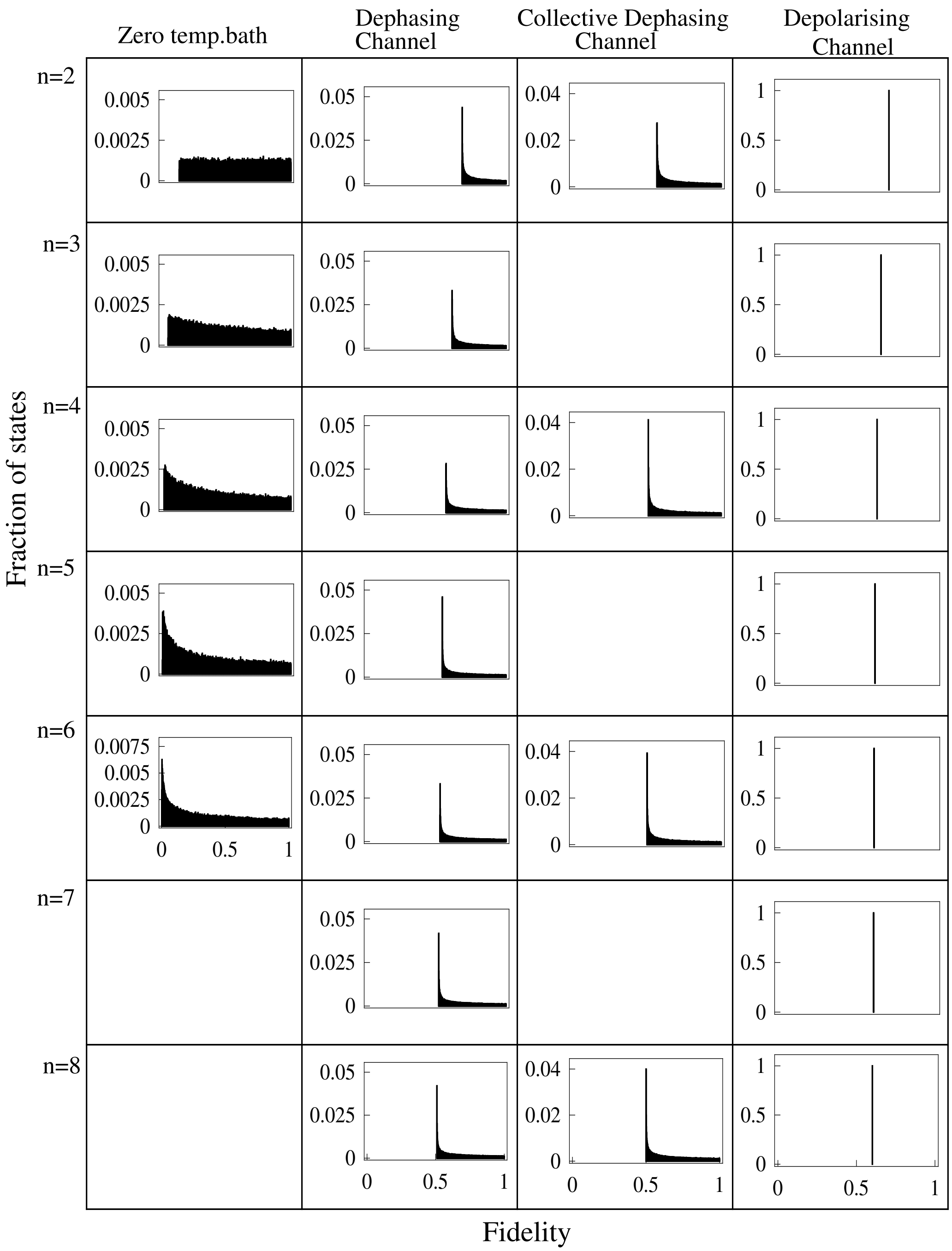

FIG. 6. Fidelity distribution of uniformly distributed random GHZ-type states as a function of system size. The variance of Fidelity distribution is maximum in case of zero temperature bath and is minimum in case of depolarising channel.The Fidelity distributions of dephasing and collective dephasing channel show similar behavior with increasing number of qubits.

computed by using Equation (16). We generate random states within the three families of states under consideration and pass them trough the depolarising channel. The fidelities are computed and the average fidelity and fidelity distributions are plotted. The average fidelity for different types of states as function of number of qubits is shown in Figure 4 while the fidelity distributions are shown in the 4th columns of Figures 5,6 & 7.

Depolarising channel is supposed to be most unbiased way of carrying out state degradation. In agreement with that view the average fidelity for the three classes of states is same and shows the same behaviors with number of qubit as is evident from Figure 4. The fidelity distribution of each set of states with increasing number of qubits also show the same pattern as can be seen from the 4th columns of Figures 5,6,&7. Furthermore there

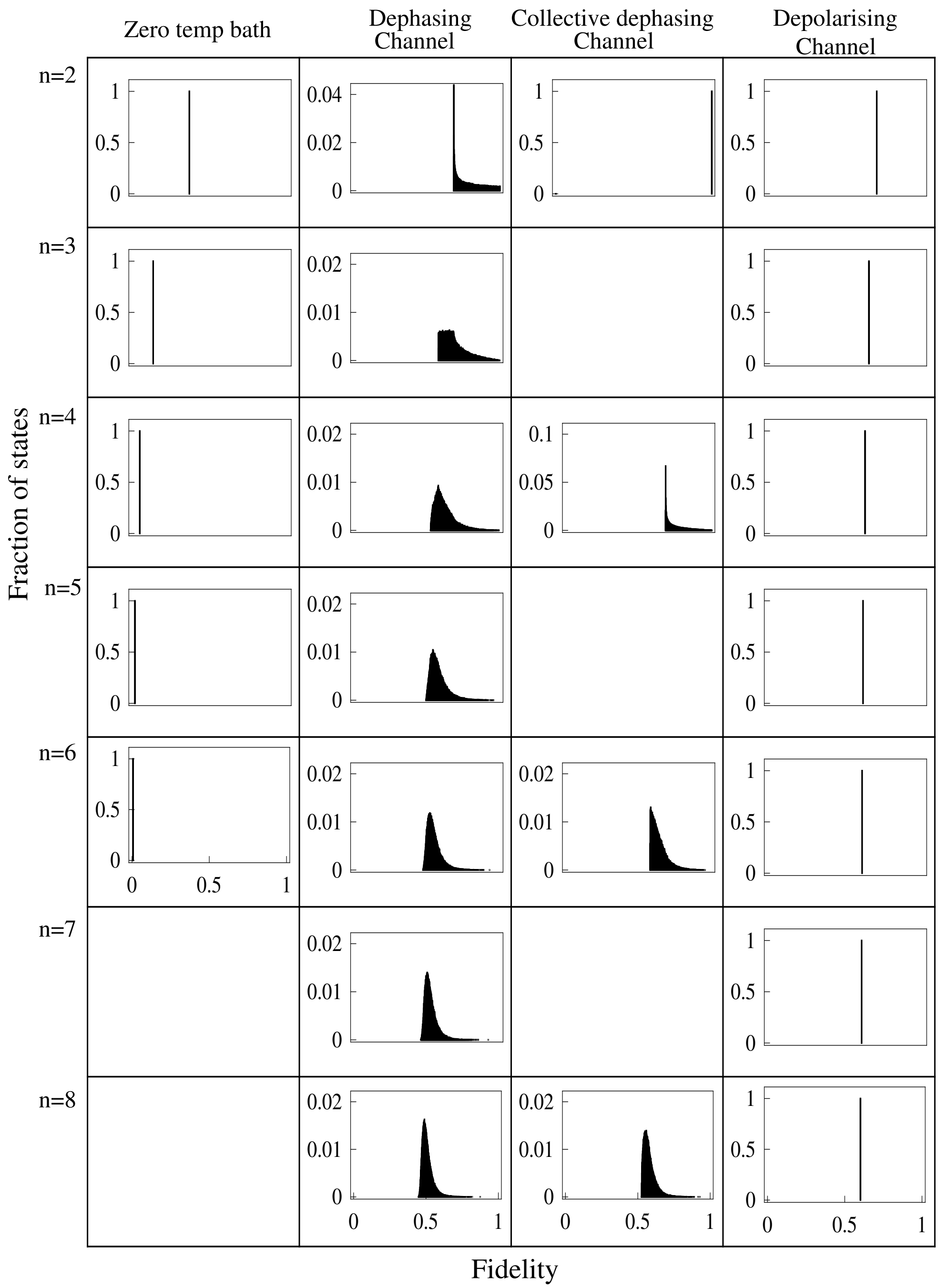

FIG. 7. Fidelity distribution of uniformly distributed random generalized W-type states as a function of system size. The variance of Fidelity distribution is zero in case of zero temperature bath model as well as depolarising channel. Fidelity distribution of w-state for zero temperature bath model shows that it is affecting all states equally.

is no variation in fidelity as is expected from from the depolarising channel.

III. COMPARISON OF FIDELITY FOR DIFFERENT CHANNELS

In the previous section, a comparison was drawn between the degeneration rates of three set of states with respect to number of qubits for all the four channels. Here, we compare the degeneration behavior of each family of states under the effect of all four channels. We have used

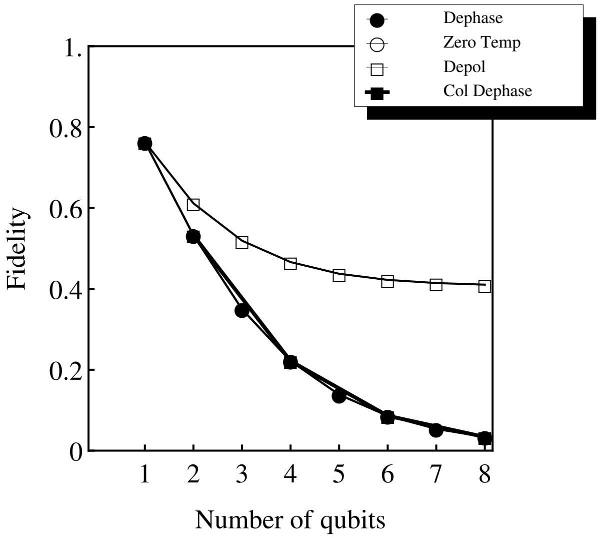

FIG. 8. Variation of average fidelity of general states as a function of system size for different channels. As we can see, the degeneration dependence on n is same for zero temperature bath, dephasing channel and collective dephasing channel. It is only the depolarising channel that effects the states in a differently.

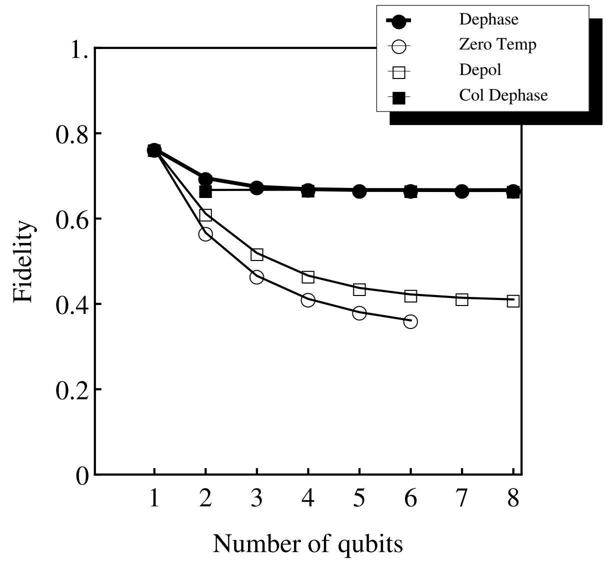

FIG. 9. Variation of average fidelity of GHZ-type states as a function of system size. While the degeneration of states is maximum in case of zero temperature bath, it is almost independent of the system size for collective dephasing channel.

the same data that was used in the previous section to draw conclusion in this section. As was mentioned on each graph in the previous section that we used specific parameter values, we used $\gamma_1 t = 1$ for zero temperature bath, $1\gamma_2 t = 2.48$ and for dephasing channel, $\Gamma t = 5$ for the collective dephasing channel and $p = 0.8348$ for the depolarising channel. These value appear arbitrary and similar behaviors will be seen for other values. The reason behind this choice is that the starting fidelities for all the channels should be same for general states. Which for zero temperature bath, dephasing channel and depolarising channel is $n = 1$ and for collective dephasing channel is $n = 2$.

A. Variation of average fidelity for general states

We consider general states and plot the average fidelity as function of no of qubits corresponding the different channels. The results are shown in Figure 8. It is clear that the dependence of degeneration on number of qubits is same for zero temperature bath, dephasing and collective dephasing channels. The states degeneration differently under the depolarisation channel where the degeneration grows slower with number qubits compared to the other cases.

B. Variation of average fidelity for GHZ-type states

Next we take GHZ states and plot their average fidelity as a function of number of qubits for different channels. The results are shown in Figure 9. The relative behavior of GHZ-type states under the effect of four channels is quite different. Figure 9 shows that degeneration of the states is least in the case of collective dephasing channel followed by dephasing channel. The graph obtained in this case is quite different from that for general states. The reason can be attributed to very small number of relative phases involved in the state. The action of zero temperature bath and depolarising channel is similar to that of general states.

C. Variation of average fidelity for W-type states

In this case we consider the average fidelity as a function of number of qubits for W-type states for different channels. The results are shown in Figure 10. It is clear from the figure that the dependence of decoherence of W-type on the number qubits is similar in the case of zero temperature bath and depolarising channel and for dephasing and collective dephasing it is similar. The decoherence effects increase more rapidly for the first two cases compared to the last two cases. This behaviors is quite different from the GHZ-type states as well as from the general states.

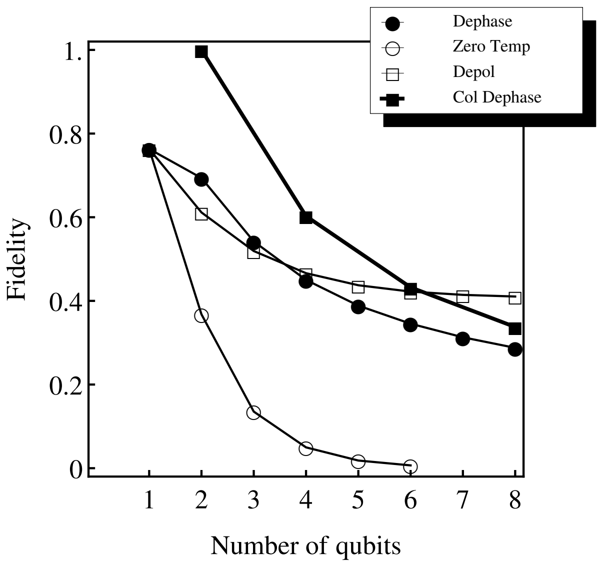

FIG. 10. Average fidelity of W-type states as a function of system size for different channels. Decay of state due to zero temperature bath is very fast, fidelity goes to almost zero for 6 qubits. The variation of the effect of dephasing channel and collective dephasing channel on the states is similar with increase in number of qubits. Depolarising channel is showing similar behavior as that for GHZ and general states.

IV. CONCLUSIONS

We studied one to eight qubit quantum systems under different zero temperature bath, dephasing channel, collective dephasing channel and depolarising channel. The main aim was to study the dependence of degradation rates on the system size which in this case was quantified by the number qubits. For each case ($n > 1$) we considered three family of states namely, the general states, GHZ-type states and W-type states and studied them for their behaviors under different environments listed above. For $n = 1$ we studied only general states. In order to draw state independent conclusions we averaged the fidelities over the family of states that we considered. We also studied the fidelity distributions.

While the average fidelity was observed to drop with increasing number qubits the three classes of states behaved differently. In case of zero temperature bath channel, degeneration rate with respect to number of qubits is maximum in the case of W-type-states and minimum in the case of GHZ-type states. On the other hand the degeneration rate for dephasing channel is minimum for GHZ-type states and maximum for general states. Depolarising channel degrades all the three sets of states in a similar way. In case of collective dephasing channel, degeneration rate of the state with respect to system size is negligible for GHZ-type state, whereas it is very similar for general states and W-type states.

We would like to clarify that we have defined GHZ-type and W-type states in a certain way. This definition is not same as GHZ-class and W-class states which are the two inequivalent classes of maximally entangled states for three qubits. Our definition is motivated by the structure of superpositions involved in the original definition of GHZ and W states. For example for two qubits for us the states $\frac{1}{\sqrt{2}}(|00\rangle \pm |11\rangle)$ will be GHZ-type while $\frac{1}{\sqrt{2}}(|01\rangle \pm |10\rangle)$ will be W-type, although they are all equivalent to each other under local transformations.

We would like to stress that we have obtained state indepdent conclusions by generating a large number of unbiased random state for each class of states that we studied. We hope that this study will help in the direction of understanding effect of non-unitary channels on different classes of states and their relative fragility for different number of qubits.

[1] M. A. Nielsen and I. L. Chuang, *Quantum Computation and Quantum Information*, quantum information, quantum computation,cryptography (Cambridge University Press, Cambridge UK, 2000).

[2] A. Z. D. Bouwmeester, Artur Ekert, *The Physics of Quantum Information* (Springer, 2000).

[3] J. E. Mooij, T. P. Orlando, L. Levitov, L. Tian, C. H. van der Wal, and S. Lloyd, Science **285**, 1036 (1999).

[4] D. Loss and D. P. DiVincenzo, Phys. Rev. A **57**, 120 (1998).

[5] J. I. Cirac and P. Zoller, Phys. Rev. Lett. **74**, 4091 (1995).

[6] B. Kane, Nature(London) **393**, 133 (1998).

[7] P. Recher and B.Trauzettel, Nanotechnology **21**, 302001 (2010), 10.1088/0957-4484/21/30/302001.

[8] J. A. Jones, Prog. Nuc. Magn. Reson. Spec. **59**, 91 (2011).

[9] T. D. Ladd, F. Jelezko, R. Laflamme, Y. Nakamura, C. Monroe, and J. L. OBrien, Nature **464**, 45 (2010).

[10] O. Gühne, F. Bodoky, and M. Blaauboer, Phys. Rev. A **78**, 060301 (2008).

[11] A. Borras, A. P. Majtey, A. R. Plastino, M. Casas, and A. Plastino, Phys. Rev. A **79**, 022108 (2009).

[12] L. Aolita, D. Cavalcanti, A. Acín, A. Salles, M. Tiersch, A. Buchleitner, and F. de Melo, Phys. Rev. A **79**, 032322 (2009).

[13] M. Ali and O. Gühne, Journal of Physics B **47**, 055503 (2014).

[14] E. Joos, H. D. Zeh, C. Kiefer, D. J. W. Giulini, J. Kupsch, and I.-O. Stamatescu, *Decoherence and the Appearance of a Classical World in Quantum Theory 2nd edition* (Springer-Verlag Berlin Heidelberg Germany, 2003).

[15] K. Kraus, *States, Effects and Operations: Fundamental Notions of Quantum Theory, Lecture Notes in Physics Vol. 190*, quantum inforamtin, quantum computation,cryptography (Springer-Verlag, New York, 1983).

[16] C. W. Gardiner and P. Zoller, *Quantum noise: A handbook of Markovian and non-Markovian quantum stochas-*

tic methods with applications to quantum optics (Springer series in synergetics) 3rd edition (Springer-Verlag Berlin Heidelberg Germany, 2004).

[17] A. R. R. Carvalho, F. Mintert, and A. Buchleitner, Phys. Rev. Lett. **93**, 230501 (2004).

[18] F. Mintert, A. R. R. Carvalho, M. Kus, and A. Buchleitner, Physics Report **415**, 207 (2005).

[19] K. Roszak and P. Machnikowski, Phys. Rev. A **73**, 022313 (2006), arxiv:quant-ph/0507027.

[20] K. Ann and G. Jaeger, Phys. Rev. B **75**, 115307 (2007).

[21] J.-M. Cai, Z.-W. Zhou, and G.-C. Guo, Phys. Rev. A **72**, 022312 (2005), arxiv:quant-ph/05040221.